PHYSICAL REVIEW E VOLUME 59, NUMBER 3 MARCH 1999

Small-angle neutron scattering study of a pressure-induced phase transition in a ternary microemulsion composed of AOT, D_2O, and *n*-decane

M. Nagao[1,]* and H. Seto[2]

[1]*Neutron Scattering Laboratory, Institute for Solid State Physics, The University of Tokyo, 106-1 Shirakata, Tokai, Naka 319-1106, Japan*

[2]*Faculty of Integrated Arts and Sciences, Hiroshima University, 1-7-1 Kagamiyama, Higashihiroshima 739-8521, Japan*

(Received 24 July 1998)

A small-angle neutron scattering experiment was carried out in order to investigate a pressure-induced phase transition in an AOT (dioctyl sulfosuccinate sodium salt)/water/*n*-decane system. The samples, 20.9%, 22.4%, and 23.0% of AOT, dissolved in an equal volume fraction of water and oil, are known to be a dense water-in-oil droplet structure at ambient temperature and pressure. With increasing pressure, a structural phase transition was observed. At higher pressure, the systems turned into two phases; a lamellar phase at the lower part of the cell and a bicontinuous phase at the upper part. A pressure dependence of the mean repeat distance for each structure was obtained. The disorder parameter both in the water-in-oil droplet structure at lower pressure and in the bicontinuous structure at higher pressure followed a unique function.
[S1063-651X(99)04103-3]

PACS number(s): 61.25.−f, 61.12.Ex, 62.50.+p, 87.16.−b

I. INTRODUCTION

Complex fluid systems, such as polymers, biological membranes, micelles, and microemulsions, have been widely investigated in order to clarify various structures they take as well as mechanisms of their self-organization. Microemulsions are typical of such systems, which are mainly composed of water, oil, and amphiphile, and in some cases alcohol or cosurfactant as a fourth or fifth component. They form various complex structures, such as water-in-oil or oil-in-water droplet, bicontinuous, lamellar, hexagonal, etc., depending on their compositions and external conditions such as temperature or pressure. Their characteristic length scales range from tens to hundreds of angstroms, thus these mixtures are generally transparent. Amphiphile molecules, being located at the oil-water interface, decrease the interfacial tension drastically, and stabilize their mesoscopic scale structures. In recent decades, microemulsion systems have been extensively investigated in view of structural formations, phase stability, self-organization processes, and interaction between ingredients [1–4].

The main parameters that characterize their structures are the amount of interfaces and the spontaneous curvature of membranes. When the concentration of amphiphiles is increased, large amounts of interfaces are formed and microemulsion structure becomes more ordered, such as hexagonal, cubic, or lamellar [5]. The concept of ‘‘spontaneous curvature’’ was first proposed by de Gennes and Taupin in 1982 [6]. A packing property of amphiphilic molecules seems to determine the spontaneous curvature of the amphiphilic layer in the first approximation. When the size of a polar head is effectively smaller than that of a hydrocarbon chain, the amphiphile layer tends to curve toward the water region. In this case, the water-in-oil droplet structure is favored. The packing property is defined not only by the ‘‘real shape’’ of molecules, but also by the hydrophile-lipophile balance (HLB) of membranes or the interaction between amphiphile molecules. Therefore, this property could be changed with varying external conditions such as temperature and/or a concentration of counterions, etc., and subsequently, a structural phase transition occurs. This hypothesis has been well confirmed by various experimental evidence of phase transitions induced by varied temperature and concentration of ingredients [7,8]. For example, a temperature-induced phase transition between bicontinuous and lamellar structure in a nonionic surfactant C_iE_j/water/oil system was investigated and its mean curvature of the amphiphile layer changed linearly from negative to positive with increasing temperature [9,10].

The structural behavior of mixtures of AOT (dioctyl sulfosuccinate sodium salt), water, and *n*-alkane has been intensively studied by many researchers, because it leads to the formation of stable one-phase dispersions over a wide range of compositions at ambient temperature and pressure without any additives. When about 20 vol % of AOT is dissolved in a mixture of water and oil at the same volume fraction, its structure at ambient temperature and pressure was verified to be a dense water-in-oil droplet by the experimental evidences of the electric conductivity and the freeze fracture electron microscopy [11,12]. Adding a small amount of salt makes the amphiphile property balanced and induces a bicontinuous structure around the HLB temperature [13]. Although small-angle x-ray (SAXS) and neutron scattering (SANS) techniques are usually suitable to find structures of microemulsions, it is not easy to distinguish from the scattering profiles whether the system takes the dense droplet structure or the bicontinuous, because the scattering profiles from the two structures are characterized only by a broad single peak. Therefore, we called the structure with a broad single peak the ‘‘microemulsion structure’’ hereafter. Details will be expressed in Sec. II.

With increasing temperature, a phase transition from the

---

*Electronic address: nagao@red.issp.u-tokyo.ac.jp droplet phase to the ordered lamellar structure has been observed in the same system [13,14]. A small-angle scattering profile from the lamellar structure is characterized by two features; one is a sharp Bragg peak originated from the stacking of membranes accompanied with some higher order peaks, and the other is a small-angle diffuse scattering originated from the concentration fluctuation of amphiphile molecules and an undulation of the lamellar membranes. Kotlarchyk *et al.* performed a SAXS measurement from the lamellar structure in the AOT system and introduced a paracrystal model [14] to interpret the observed scattering profiles; they assumed that the lamellar structure contains a randomly oriented assembly of lamellar microdomains or stacks. Although their model could explain the SAXS profiles from samples with small water-to-surfactant ratio, the scattering profile with large water-to-surfactant ratio was poorly explained. A more convincing model proposed by Nallet *et al.* [15] will be explained in Sec. II.

Although pressure is an important physical parameter for structural formation of various systems, few experiments have been done because the experimental technique is rather difficult compared with other techniques, for example, temperature variation. Eastoe *et al.* investigated pressure effects on phase behavior of various droplet microemulsion systems by means of SANS and dynamical light scattering (DLS) [16]. For AOT systems, the effect of pressure depends on the kind of *n*-alkane; for alkanes whose carbon number $C \geqslant 6$, phase boundaries on the P-T phase diagram have a negative slope, while for $C<6$, phase boundaries have a positive slope. This means that increasing pressure plays the same role as increasing temperature for the case of $C \geqslant 6$, however the effect is opposite for $C<6$. They also reported a pressure dependence of the size of droplets for various water-in-oil droplet microemulsion systems [17]. It tends to increase with increasing pressure for nonionic surfactant systems, while it is independent of pressure for ionic surfactant systems. A similar experiment was done by Fulton and Smith for an AOT/water/supercritical propane [18]. They showed that the different compressibilities of water, oil, and amphiphiles are an origin of the structural changes under pressure variation experiments. Saïdi *et al.* investigated a pressure-induced percolation phenomenon in an AOT/water/undecane system by means of an electrical conductivity measurement and a cloud point method [19]. They claimed that the feature of the pressure-induced percolation is quite similar to the temperature-induced percolation [11]. They determined a P-ϕ phase diagram, which was essentially the same as the T-ϕ phase diagram given by Cametti *et al.* [11], where ϕ is the volume fraction of water and surfactant against the whole volume and corresponds to the number density of droplets. Therefore, they suggested that the high-pressure phase is the ordered lamellar as the case of the high-temperature phase [19]. Recently, Nagao *et al.* have shown experimental evidence of SANS that the dense water-in-oil droplet phase of an AOT/water/*n*-decane system transformed to the ordered lamellar structure by applying pressure [20]. They confirmed that pressure induces the same phase transition as temperature, however they indicated that the pressure dependence of the characteristic repeat distance was different from the temperature dependence.

In this paper we describe further SANS results on the pressure-induced phase transition, from the dense water-in-oil droplet to the lamellar structure. We have found that at higher pressure, the system is in a two-phase with a lamellar structure at the lower part of the cell and a bicontinuous structure at the upper part. Pressure dependences of two characteristic length scales, the mean repeat distance d and the correlation length ξ, were obtained from the measured scattering profiles. The pressure dependence of a disorder parameter $D(\propto d/\xi)$, of both the lower and the higher pressure phases, could be normalized to fall into a unique function for all the samples investigated.

II. THEORY

In order to explain the broad single peak profile of small-angle scattering from the ''microemulsion structure,'' Teubner and Strey proposed a simple function derived from an expansion of a phenomenological Ginzburg-Landau free energy [21]. The microemulsion structure is characterized by an alternative distribution of water and oil domains, for which they introduced the following spatial correlation function:

$$\gamma(r)=\frac{d_m}{2\pi r}\exp\left[-\frac{r}{\xi_m}\right]\sin\left(\frac{2\pi r}{d_m}\right), \tag{1}$$

where the parameters d_m and ξ_m are the mean repeat distance between water (oil) domains and the correlation length, respectively. The suffix ''m'' means a value characterizing the microemulsion structure. From the Fourier transformation of the correlation function, a scattering function was calculated as

$$I(Q)=\frac{1}{A+BQ^2+CQ^4}. \tag{2}$$

In their model, the d_m and ξ_m are obtained from the fitting parameters A, B, and C using the formulas

$$d_m=2\pi\left\{\frac{1}{2}\left[\left(\frac{A}{C}\right)^{1/2}-\frac{B}{2C}\right]\right\}^{-1/2}, \tag{3}$$

$$\xi_m=\left\{\frac{1}{2}\left[\left(\frac{A}{C}\right)^{1/2}+\frac{B}{2C}\right]\right\}^{-1/2}. \tag{4}$$

Although the scattering function is quite simple, it could explain many experimental results successfully [3,13,22]. Chen *et al.* proposed a disorder parameter $D_m=d_m/2\pi\xi_m$ in order to estimate the degree of polydispersity in the size of oil or water domains. They predicted that the droplet structure can be identified if the parameter D_m is less than $D_0=0.446$ in distinction from that of the bicontinuous structure, empirically [22].

There are some other models that take the place of Teubner and Strey's models, for example, Gompper and Schick's theory [23] and the modified Berk random wave model [24]. The former is based on a lattice model of microemulsion and explained in SANS profiles at a higher-Q region better than Teubner and Strey's model, because the higher order of the free energy functional is included [23]. In their model, the two characteristic length scales d_m and ξ_m are obtained as in the case of Teubner and Strey. The latter model, proposed by

Choi and Chen [24], extended Teubner and Strey's model by including a third characteristic length scale. This model could explain the SANS profile from the bicontinuous structure in better fashion, incorporating the average mean curvature and the Gaussian curvature of the interface. In their model, however, the Gaussian curvature was determined to be always negative, therefore it cannot be applied to the droplet structure. Because Teubner and Strey's model is more general to explain both the bicontinuous and the droplet structure, we find that it is more appropriate to use this model to analyze the present successive structural change.

A model proposed by Nallet *et al.* is useful to explain SANS profiles from the lamellar structure [15]. In their theory, the scattering from the lamellar structure consists of two parts: one is the quasi-Bragg peak due to the stacking of the lamellar membranes and the other is small-angle diffuse scattering originating from the concentration fluctuation of amphiphile molecules as described in Sec. I. They assumed that the lamellar structure is stabilized by the short-range (hydration and screened electrostatic) interactions as well as the long-range (van der Waals and electrostatic) interactions. The lamellar membranes are assumed to be characterized by the Helfrich elastic energy density [25]. Their theory is applicable to perfectly oriented dilute lamellar structures. By their model, many physical constants can be calculated from the scattering profiles by fitting to their equation, although it requires high-resolution spectroscopy. Unfortunately, the Q resolution of neutron scattering experiments is not always sufficient for this purpose. Therefore they simplified the theoretical description using a Lorentzian form [15] for the z direction which is perpendicular to amphiphile layers,

$$I(Q)=\frac{E}{Q^2\xi_\rho^2+1}+\frac{F}{(Q-Q_0)^2\xi_l^2+1}, \tag{5}$$

where Q_0, ξ_ρ, and ξ_l are the center of a first-order peak, the correlation length of the concentration fluctuation of amphiphilic molecules, and the spatial correlation length of the lamellar membranes, respectively. The first term represents the small-angle diffuse scattering and the second represents the quasi-Bragg scattering corresponding to the stacking of the lamellar membranes. The periodic repeat distance of the lamellar membranes d_l can be given by $d_l=2\pi/Q_0$.

III. EXPERIMENT

The AOT used was purified before mixing by a method from Kunieda and Shinoda [26]; after removing excess oil from 99% of AOT purchased from Sigma, the purified AOT was extracted with benzene. The 99% of D_2O and 99.9% of *n*-decane were purchased from Isotec Inc. and Katayama Chemical Company, respectively, and used without further purification. An equal volume fraction of water and oil was mixed with AOT at volume fractions $\phi_s=0.209$, 0.224, and 0.230. These mixtures were known to be dense water-in-oil droplet structures at ambient temperature and pressure.

The samples were contained in a high-pressure cell for SANS [27]. The main body of the cell was made of stainless steel. Two 20-mm-thick truncated cone-shape sapphires were used as windows in order to pass the neutron beam and to keep the sample inside against the pressure. The sapphires were tightly held by stainless rings directly. Two copper rings and one Teflon ring including powdered copper were placed between a sapphire holder ring and the main body. The sample thickness can be changed from 0.3 to 1.5 mm with a Cu metal spacer. In our experiments, 0.3 and 0.5 mm spacers were used to optimize the scattering intensity. A pressure was applied to the sample through a 1:1 free piston through a hand pump. Kerosene was used as the pressurizing liquid. The pressure was measured with a 6 in. Heise gauge with an accuracy of ±0.5 MPa. The high-pressure cell was covered with an aluminum thermal shield with a quartz window in order to avoid temperature fluctuations. All the measurements were performed under constant room temperature of $T=297.7\pm0.5\,\mathrm{K}$.

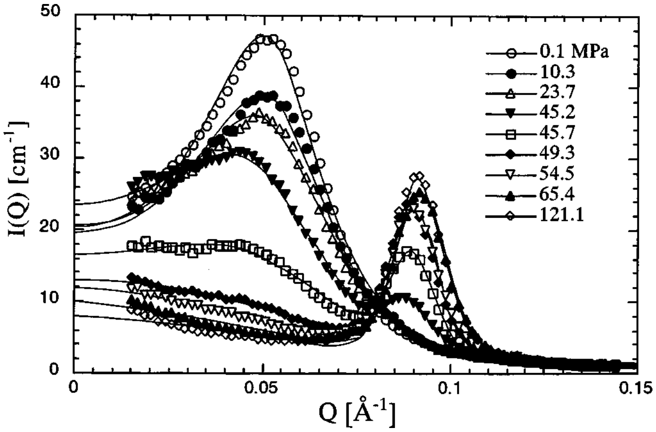

FIG. 1. SANS profiles for the sample $\phi_s=0.224$ at various pressures. A peak at lower Q corresponds to the dense water-in-oil droplet structure and the peak at higher Q represents the lamellar structure. The peak position of lower Q shifted with increasing pressure and the peak height decreased; subsequently the peak at the higher Q grew above 45 MPa. The lines are the results of fitting (see text).

SANS experiments were carried out at the SANS-U spectrometer in JRR-3M of Japan Atomic Energy Research Institute (JAERI), Tokai [28]. The 7 Å incident cold neutron beam was mechanically selected with a resolution of 10%. A two-dimensional position sensitive detector was placed 2 m from the sample position in order to cover the momentum transfer range of $0.015\leqslant Q\leqslant0.144\,\text{Å}^{-1}$. All the measured data were calibrated to an absolute intensity with a Lupolen standard.

IV. RESULTS

In Fig. 1, a typical pressure variation of SANS profiles for a sample $\phi_s=0.224$ is shown. Two-dimensional data were radially integrated to represent an average feature independent of directions. The tendency of the change of the profile with increasing pressure was qualitatively the same as what Nagao *et al.* have shown before [20]. At ambient pressure a broad peak existed at $Q\sim0.05\,\text{Å}^{-1}$. With increasing pressure, this peak shifted a little to higher Q up to $P_s=8.7\,\mathrm{MPa}$ (P_s is defined as the transition start pressure) and moved to lower Q above P_s and gradually vanished. At 45.2 MPa, a new sharp peak appeared at $Q\sim0.09\,\text{Å}^{-1}$ and it successively grew with increasing pressure. Above $P_f=50.5\,\mathrm{MPa}$ (P_f represents the transition finish pressure), a

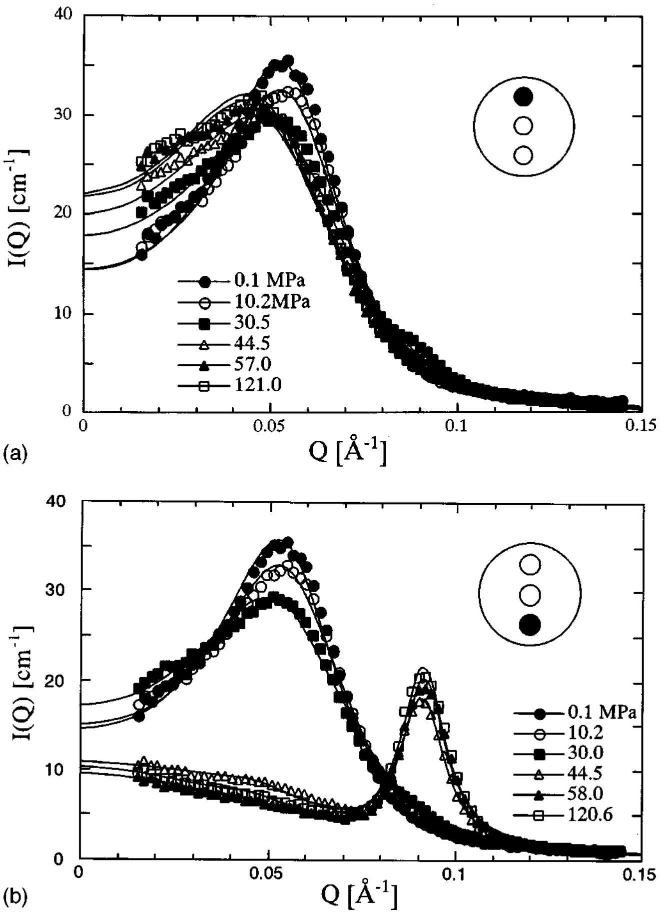

FIG. 2. (a) SANS profiles from the upper part of the sample $\phi_s = 0.230$ at various pressures. There are no lamellar Bragg peaks except for the slight shoulder at around 30 MPa. The main peak decreases a little below 30 MPa, on the other hand it increased with pressure above 30 MPa. (b) SANS profiles at the lower part. A quasi-Bragg peak corresponding to the lamellar structure above 40 MPa was observed around $Q \sim 0.09\,\text{Å}^{-1}$. The inset indicates the cell window and the neutron beam position (full circle).

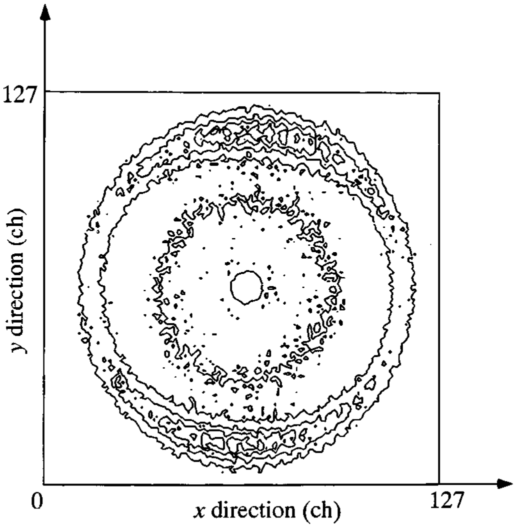

FIG. 3. A contour map of the SANS profile obtained from the lamellar structure of the sample $\phi_s = 0.224$ at $P = 100$ MPa. The y axis is parallel to the gravity. The peak intensity in the y direction was higher than that in the x direction. This tendency is the same for all the samples of the lamellar structure. Units along the x and y directions are the channel number of the two-dimensional detector, respectively.

slight increase of the lamellar peak was observed. The same behavior was observed for all the samples. The broad single peak from the low-pressure phase could be explained by Teubner and Strey's formula [Eq. (2)]. The SANS profile from the high-pressure phase could be successfully fitted by the equation proposed by Nallet *et al.* [Eq. (5)]. At a transient phase between P_s and P_f, a linear combination of Eqs. (2) and (5) was utilized in order to explain the observed profile which must contain both the microemulsion and the lamellar structure. Solid lines in Figs. 1 and 2 are the results of fitting to these equations.

In order to check whether each phase was uniform or not, lower and upper parts of the samples were irradiated by neutron beams separately. Because the aperture of the high-pressure cell is 20 mm, and the neutron beam size was selected to be 3 mm, we focused on a position 5 mm from the top of the window as the upper part, and on 5 mm from the bottom as the lower part. [See the insets in Figs. 2(a) and 2(b).] The pressure dependences of the SANS profile from both the upper and the lower part for the sample of $\phi_s = 0.230$ are shown in Figs. 2(a) and 2(b), respectively. Below P_s these profiles were essentially the same, i.e., the low-pressure phase is a single phase. Above P_s the scattering profiles at the lower and the upper part became different. At $P = 44.5$ MPa, a sharp peak around $Q \sim 0.09\,\text{Å}^{-1}$ was observed from the lower part, while not from the upper. With increasing pressure, the sharp peak at the lower part grew slightly above 44.5 MPa. [See Fig. 2(b).] In this process, the broad peak originated from the low-pressure phase decreased monotonously and vanished completely at P_f ($= 48.8$ MPa). On the other hand, at the upper part, the broad peak did not disappear up to the highest pressure we reached. [See Fig. 2(a).] The peak position shifted a little to lower Q up to $P = P_f$, at the same time a broadening of the peak was observed. At 30.5 MPa (slightly above P_s). a small shoulder appeared around $Q = 0.09\,\text{Å}^{-1}$, which might correspond to the lamellar structure, however the shoulder did not grow further and vanished above this pressure. All the profiles from the upper part seem essentially the same except for the small shoulder, and they could be explained by Teubner and Strey's formula [Eq. (2)].

The scattering pattern of the high-pressure lamellar structure obtained with the two-dimensional neutron counter is shown in Fig. 3. The y direction is parallel to the direction of gravity. It clearly shows that the intensity of the lamellar peak along the y direction is higher than that along the x direction. This tendency is the same for all the samples in the lamellar structure. In Fig. 4, intersections of Fig. 3 through the beam center along the x and y axes are shown. The solid line indicates the fit result to Eq. (5). In Table I the resultant fit parameters are given. The Bragg peak position Q_0 was almost the same, however the peak height F along the y direction was larger than that along the x direction. On the other hand, the low-Q diffuse scattering characterized by E and ξ_ρ was the same within error bars, both along the x and y axes. This means that the concentration fluctuation of the amphiphile molecules did not depend on the direction. The difference of the profiles between the x and y axes is only the

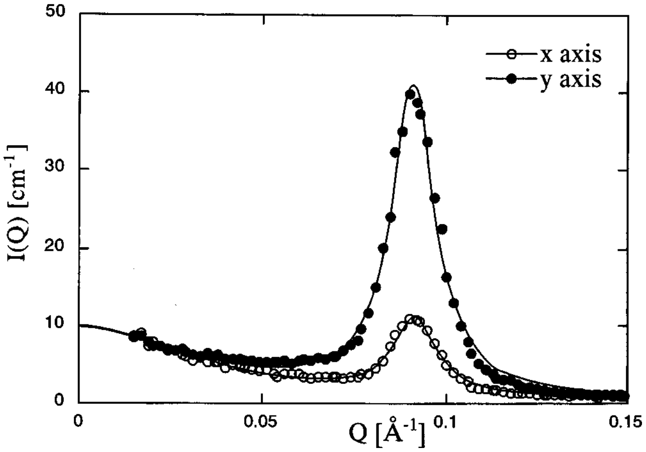

FIG. 4. Intersections of the profile given in Fig. 3 along the *x* and *y* axes through the beam center are shown. Solid lines indicate the results of fitting to the formula proposed by Nallet *et al.* [Eq. (5)].

peak height of the Bragg peak of the lamellar membranes. This means that the structure in the lamellar phase was essentially the same for each direction except for the degree of stacking of the membranes. Therefore, all the data could be radially averaged to reveal an averaged structural feature. The reason for the anisotropy of the Bragg peak will be discussed in Sec. V.

It is difficult to separate the scattering profiles of the lamellar structure from that of the microemulsion in the transient phase between P_s and P_f, because the low-Q diffuse scattering from the lamellar structure cannot easily be separated from the broad peak of the microemulsion structure. Therefore, we analyzed them by assuming that a ratio of the two terms in Eq. (5), i.e., the ratio of the intensity of the low-Q diffuse scattering (E) to that of the quasi-Bragg peak (F), was kept constant even in the transient phase.

From these procedures, the pressure dependences of the characteristic mean repeat distances d_m and d_l for both the microemulsion structure (subscript m) and the lamellar structure (subscript l) were obtained as shown in Fig. 5. With increasing pressure, the d_m gradually decreased below P_s, subsequently it increased between P_s and P_f, and finally it remained constant above P_f. Above P_s, the lamellar structure appeared and the d_l was about 75 Å. It decreased slightly with increasing pressure and arrived at a constant value, $d_{lf} = 69$ Å at P_f. In Fig. 6, the ϕ_s dependence of d_{m0}, which is d_m at ambient pressure, d_{lf} above P_f, and in addition to the ϕ_s dependence of P_s are summarized. In order to explain the ϕ_s dependence of the d_{m0}, a phenomenological explanation of the droplet structure was proposed by Kotlarchyk *et al.* [29]. They assumed that water droplets coated by an AOT monolayer dispersed in oil and formed a densely packed structure like a cubic phase. They derived a relation between d_{m0} and ϕ_s as follows:

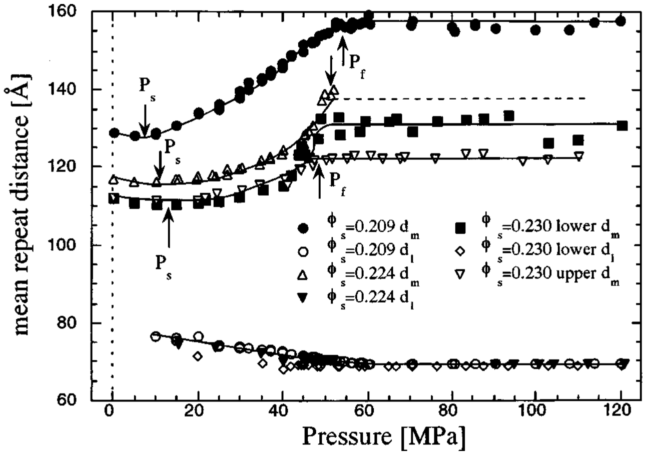

FIG. 5. The pressure dependence of both the d_m and the d_l for all the samples measured. The d_m depends on both pressure and ϕ_s, while the d_l does not depend on ϕ_s. The lines are a guide for the eyes.

$$d_{m0} = 2\pi \frac{\Delta}{2.25} \frac{(1-\phi_s)^{2/3}}{\phi_s}, \tag{6}$$

where Δ is the molecular length of AOT defined by the ratio of the steric volume of an AOT molecule to the average head group area. The solid line in Fig. 6 indicates the result of fitting. The obtained value $\Delta = 13.7 \pm 0.1$ Å was consistent with the value in the literature [29]. The d_{lf} was independent of the ϕ_s, and this behavior was completely different from the temperature-induced phase transition, in which the characteristic repeat distance of the lamellar structure decreased with increasing ϕ_s [30].

In order to clarify the structure of the microemulsion, which was found at low pressure and in the upper part at high pressure, the disorder parameter D_m ($= d_m/2\pi\xi_m$) was calculated. It is remarked that the D_m at low pressure was below $D_0 = 0.446$, and at $P > P_s$ the D_m went above D_0. This result confirmed that the low-pressure phase is the droplet structure and in the upper part at high pressure it is bicontinuous. In Fig. 7, the pressure dependence of D_m is summarized as a function of the biased pressure P-P_s. The D_l($= d_l/2\pi\xi_l$) for the lamellar is also shown. All the curves seem to fall into a unique curve both for the microemulsion and the lamellar structure.

From these results, the pressure-induced phase transition is summarized as follows. With increasing pressure from ambient pressure, the droplet structure becomes disordered.

TABLE I. Result of the fitting to Eq. (5) for the scattering profiles of the lamellar of the *x* and *y* directions for the sample $\phi_s = 0.224$ at $P = 100$ MPa.

	E (cm^{-1})	ξ_ρ (Å)	F ($\times 10^{-3}$ cm^{-1})	ξ_l (Å)	Q_0 (Å^{-1})
x axis	9.7±0.2	25.5±0.8	9.9±0.2	145±4	0.0912±0.0001
y axis	9.6±0.7	26.3±2.5	39.6±0.5	137±3	0.0910±0.0001
radially averaged	10.0±0.5	26.7±1.7	28.5±0.4	139±3	0.0912±0.0001

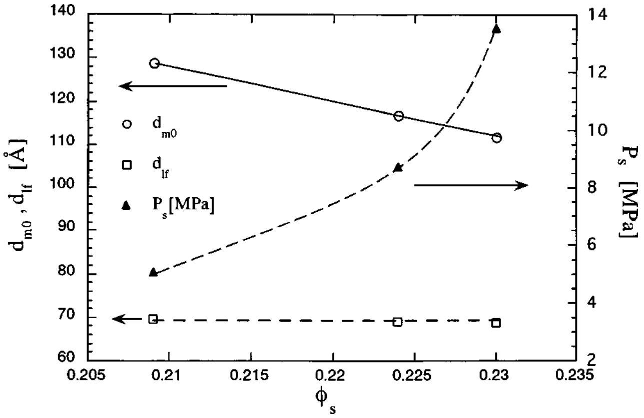

FIG. 6. The ϕ_s dependence of the d_{m0} at ambient pressure and d_{lf} for the lamellar phase above P_f and P_s are shown. The solid line indicates the result of fitting to Eq. (6). The dashed lines are a guide for the eyes.

When the pressure crosses the P_s, the lamellar structure appears and the rest of the sample becomes disordered bicontinuous. Between P_s and P_f, the lamellar structure grows at the lower part. However, between P_s and P_f, the upper part remains bicontinuous and becomes more disordered, and finally above P_f, the system is stabilized as the coexistence of the lamellar and the bicontinuous structure.

V. DISCUSSION

Below P_s, the mean repeat distance between droplets, d_m, decreases with increasing pressure. A similar behavior was observed with increasing temperature [30], which could be understood taking the experimental result in a dilute droplet system presented by Kotlarchyk *et al.* [31] into consideration. They indicated that the radius of droplets decreased with increasing temperature. Because the volumes of ingredients are conserved, a number of droplets increases with increasing temperature, and the d_m should decrease. Therefore, we argue that the same process occurred in the case of the pressure variation. At $P=P_s$, small domains of lamellar structure appear everywhere in the low-pressure phase matrix, and it turns out to coexist with the microemulsion. Subsequently between P_s and P_f, the lamellar domains grow in size gradually with increasing pressure and fall down toward the lower part of the cell because of gravity. The upper part at high pressure loses amphiphile molecules in the transition process; its ϕ_s decreases effectively and the d_m increases. Above P_f, both the d_m and the d_l are kept constant. If the mean distance between membranes in the lamellar structure is determined by the thermodynamic condition of the Helfrich repulsion (discussed below), it remains almost the same independent of ϕ_s.

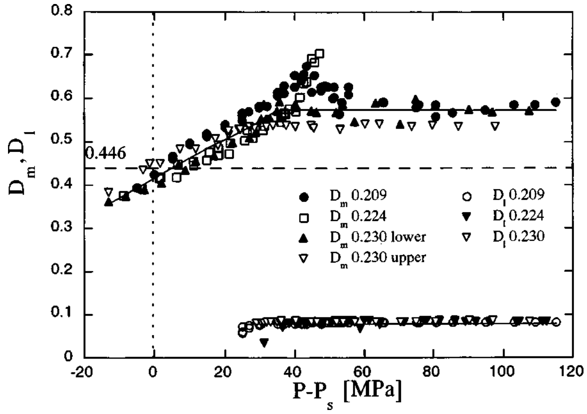

FIG. 7. The pressure dependence of the disorder parameter D for all the samples measured. The D_m's are the disorder parameters obtained from the microemulsion structure, and the D_l's are from the lamellar structure. The numbers at the legend mean the values of ϕ_s. For $\phi_s=0.230$, the scattering from the lower part included both features of the lamellar and the ''microemulsion'' structures even above P_f. All the data seem to fall into a unique curve (the solid line is a guide for the eyes). The horizontal axis indicates the biased pressure P-P_s.

The pressure dependence of the disorder parameter D is quite impressive in the present results. Although the name of D is ''disorder parameter,'' it is not an inverse of the order parameter, because the latter is a conserved quantity. If we select the surfactant concentration ϕ_s as an order parameter following some other previous works [32], the phase separation into the surfactant rich phase and the poor phase can be explained. However, we believe that the D must express a degree of ''disorder'' in some sense. Because the D is extracted from a profile of a correlation peak around $Q=0.05\,\text{Å}^{-1}$, it must be reflected by a degree of ''disorder'' in this semimicroscopic length scale of about 100 Å. Thus we argue that the ''disorder parameter'' D_m for the microemulsion structure can be interpreted as an inverse of a ''semimicroscopic order parameter.'' This is the reason why the observed D_m's for all the samples could fall into a unique function using only one parameter P_s.

In the present study, the anisotropic quasi-Bragg scattering from the stack of membranes and the isotropic diffuse scattering from the concentration fluctuation were observed from the lamellar structure. So far, the anisotropy of the diffuse scattering has been discussed in connection with an interaction between membranes that stabilize the lamellar structure. In the binary AOT/water system, the lamellar structure is believed to be stabilized by electrostatic forces between membranes [33,34]. In such a case, anisotropic small-angle diffuse scattering perpendicular to the membranes was observed. This is because the electrostatic interaction tends for the membranes to be flat and the density of amphiphile molecules can fluctuate within the membranes. On the other hand, in the case where the Helfrich repulsion mainly stabilizes the lamellar structure, the concentration fluctuation of amphiphile molecules is governed by the flexibility of the membranes [15]. If membranes are flexible enough, they undulate easily and the diffuse scattering becomes isotropic. In the present ternary microemulsion case, the diffuse scattering is isotropic although the lamellar membranes are oriented with its normal axis almost parallel to gravity. This result indicates that the Helfrich repulsion stabilizes the lamellar stacking in this system.

In general, an isotropic quasi-Bragg scattering from the lamellar structure of the ternary microemulsion system is observed unless microdomains of the lamellar are oriented by some method, for example, using a sample holder full of thin quartz plates [15]. It is known that long molecules, for example liquid crystal, can be aligned to a surface of a glass plate. Therefore, we have checked the effect of the thickness of a sample cell on the anisotropy of the quasi-Bragg scattering by a temperature-induced lamellar structure, because it was difficult to make the sample cell thicker than 1.5 mm using the high-pressure cell. We could observe a slight anisotropic quasi-Bragg scattering from the sample of 1 mm^t, however an isotropic scattering was observed from the 2 mm^t sample. From these results, we can conclude that the anisotropic quasi-Bragg scattering from the high-pressure lamellar phase was due to the interaction between sapphire windows and the sample inside.

As described in Sec. I, phase transitions among various semimicroscopic structures occur when the hydrophile-lipophile balance (HLB) of amphiphile changes with varying external conditions. In the case of AOT, amphiphile membranes favor to curve toward water, and the water-in-oil droplet structure is formed at ambient temperature and pressure. Normally, the nature of an ionic amphiphile is changed from lipophilic to hydrophilic by increasing temperature because the dissociation of the counterion in the head group will increase. Thus the spontaneous curvature approaches zero, the amphiphile membrane favors to be flat, and the lamellar structure is stabilized. In the case of a pressure-induced phase transition, it is natural to interpret that pressure affects the HLB, the spontaneous curvature changes, and phase transition occurs. Actually, Eastoe *et al.* showed that the effect of pressure on the phase behavior was the same as that of temperature in the case of $C=10$ (*n*-decane) [16]. However, the origin of the pressure effect on HLB must not be the same as that of temperature. As described in Sec. I, the pressure dependence of phase behavior was not the same for the cases where the carbon number of alkane is less than 6 or above 6. This evidence showed that an interaction between lipophilic tails of AOT and oil molecules should also be considered in order to understand the effect of pressure on the phase transition. This may be the reason why the ϕ_s dependence of the d_{lf} was different from the case of the temperature-induced lamellar. We believe that not only the interaction between water and amphiphile but also the interaction between amphiphile and oil molecules should be considered to understand the pressure-induced phase transition. Because the difference between these two phase transitions is important, the details will be discussed in our following paper [30].

VI. CONCLUSION

In this work, pressure-induced phase transition from the dense water-in-oil droplet structure to the coexistence phase of the bicontinuous and the lamellar was confirmed by means of small-angle neutron scattering. The high-pressure lamellar phase existed at the lower part, while the bicontinuous microemulsion existed at the upper part. The pressure dependences of the mean repeat distance in both the microemulsion phase (d_m) and the lamellar phase (d_l) were obtained. The disorder parameter D's for all the samples measured can fall into a unique function of P-P_s. Below P_s, the system formed a dense water-in-oil droplet microemulsion and the interdroplet distance decreased with increasing pressure. Above P_s, the lamellar structure appeared and the rest of the system became bicontinuous.

ACKNOWLEDGMENTS

We appreciate Professor S. Komura at Ochanomizu University for his critical reading of the manuscript and Professor H. Okabayashi at Nagoya Institute of Technology for supplying the purified AOT. We thank the staff at the Neutron Scattering Laboratory, Institute for Solid State Physics, and D. Okuhara at Hiroshima University for supporting the SANS experiments. The SANS experiments were done under the approval of the Neutron Scattering Program Advisory Committee (Proposal No. 97-136). One of the authors (H.S.) was supported by a Grant-in-Aid for Scientific Research (No. 07740329) from the Japanese Ministry of Education, Science and Culture.

[1] See, for example, N. Boden, P. J. B. Edwards, and W. Jolley, in *Structure and Dynamics of Strongly Interacting Colloids and Supramolecular Aggregates in Solution*, edited by S. H. Chen, J. S. Huang, and P. Tartaglia (Kluwer Academic, Dordrecht, 1989), pp. 433–461.
[2] M. Kahlweit and R. Strey, Angew. Chem. Int. Ed. Engl. **24**, 654 (1985).
[3] S. Komura, H. Seto, T. Takeda, M. Nagao, Y. Ito, and M. Imai, J. Chem. Phys. **105**, 3264 (1996).
[4] D. Langevin, Acc. Chem. Res. **21**, 255 (1988).
[5] E. W. Kaler, H. T. Davis, and L. E. Scriven, J. Chem. Phys. **79**, 5685 (1983).
[6] P. G. de Gennes and C. Taupin, J. Phys. Chem. **86**, 2294 (1982).
[7] M. Kahlweit, R. Strey, D. Haase, H. Kunieda, T. Schmeling, B. Faulhaber, M. Borkovec, H. F. Eicke, G. Busse, F. Eggers, TH. Gunck, H. Richmann, L. Magid, O. Söderman, P. Stilbs, J. Winkler, A. Dittrich, and W. Jahn, J. Colloid Interface Sci. **118**, 436 (1987).
[8] J. Eastoe and R. K. Heenan, J. Chem. Soc., Faraday Trans. **90**, 487 (1994).
[9] D. D. Lee and S. H. Chen, Phys. Rev. Lett. **73**, 106 (1994).
[10] S. K. Ghosh, S. Komura, H. Seto, J. Matsuba, T. Takeda, M. Hikosaka, and M. Imai, Prog. Colloid Polym. Sci. **106**, 98 (1997).
[11] C. Cametti, P. Codastefano, P. Tartaglia, J. Rouch, and S. H. Chen, Phys. Rev. Lett. **64**, 1461 (1990).
[12] W. Jahn and R. Strey, J. Phys. Chem. **92**, 2294 (1988).
[13] S. H. Chen, S. L. Chang, and R. Strey, J. Chem. Phys. **93**, 1907 (1990).
[14] M. Kotlarchyk, E. Y. Sheu, and M. Capel, Phys. Rev. A **46**, 928 (1992).
[15] F. Nallet, D. Roux, and S. T. Milner, J. Phys. (France) **51**, 2333 (1990).
[16] J. Eastoe, B. H. Robinson, and D. C. Steytler, J. Chem. Soc., Faraday Trans. **86**, 2883 (1990).
[17] J. Eastoe, D. C. Steytler, B. H. Robinson, and R. K. Heenan, J.

Chem. Soc., Faraday Trans. **90**, 3121 (1994).

[18] J. L. Fulton and R. D. Smith, J. Phys. Chem. **92**, 2903 (1988).

[19] Z. Saïdi, J. L. Daridon, and C. Boned, J. Phys. D **28**, 2108 (1995).

[20] M. Nagao, H. Seto, S. Komura, T. Takeda, and M. Hikosaka, Prog. Colloid Polym. Sci. **106**, 86 (1997); M. Nagao, H. Seto, D. Okuhara, H. Okabayashi, T. Takeda, and M. Hikosaka, Physica B **241–243**, 970 (1998).

[21] M. Teubner and R. Strey, J. Chem. Phys. **87**, 3195 (1987).

[22] S. H. Chen, S. L. Chang, R. Strey, J. Samseth, and K. Mortensen, J. Phys. Chem. **98**, 7427 (1991); S. H. Chen, S. L. Chang, and R. Strey, Prog. Colloid Polym. Sci. **81**, 30 (1990).

[23] G. Gompper and M. Schick, Phys. Rev. B **41**, 9148 (1990).

[24] S. M. Choi and S. H. Chen, Prog. Colloid Polym. Sci. **106**, 14 (1997); S. H. Chen and S. M. Choi, J. Appl. Crystallogr. **30**, 755 (1997).

[25] W. Helfrich, Phys. Lett. **43A**, 409 (1973); W. Helfrich, Z. Naturforsch. A **33**, 305 (1978).

[26] H. Kunieda and K. Shinoda, J. Colloid Interface Sci. **70**, 577 (1979).

[27] H. Takeno, M. Nagao, Y. Nakayama, H. Hasegawa, T. Hashimoto, H. Seto, and M. Imai, Polym. J. (Tokyo) **29**, 931 (1997).

[28] Y. Ito, M. Imai, and S. Takahashi, Physica B **213&214**, 889 (1995).

[29] M. Kotlarchyk, S. H. Chen, J. S. Huang, and M. W. Kim, Phys. Rev. Lett. **53**, 941 (1984); S. H. Chen, D. Lee, and S. L. Chang, J. Mol. Struct. **296**, 259 (1993).

[30] M. Nagao, H. Seto, D. Okuhara, and Y. Matsushita, J. Phys. Chem. Solids (to be published); M. Nagao, Y. Kawabata, H. Seto, T. Takeda, S. Komura, and Y. Matsushita, *Slow Dynamics in Complex Systems*, edited by M. Tokuyama and I. Oppenheim (American Institute of Physics, New York, in press).

[31] M. Kotlarchyk, S. H. Chen, J. S. Huang, and M. W. Kim, Phys. Rev. A **29**, 2054 (1984).

[32] S. K. Ghosh, S. Komura, J. Matsuba, H. Seto, T. Takeda, and M. Hikosaka, Jpn. J. Appl. Phys., Part 1 **37**, 919 (1998).

[33] See, for example, D. Roux, C. R. Safinya, and F. Nallet, in *Micelles, Membranes, Microemulsions, and Monolayers*, edited by W. M. Gelbert, A. Ben-Shaul, and D. Roux (Springer-Verlag, New York, 1994).

[34] P. Ekwall, L. Mandell, and K. Fontell, J. Colloid Interface Sci. **33**, 215 (1970).